

Analysis of a high-power laser thermal phenomena induced onto a composite made UAV/drone in flight

DAN SAVASTRU, VALERIU SAVU*, MĂDĂLIN ION RUSU*, MARINA TAUTAN, ALEXANDRU STANCIU
National Institute R&D of Optoelectronics Inoe 2000, 409 Atomistilor Str., Magurele, Ilfov, Romania

Nowadays there is an increased interest in countering military drones/UAVs in flight. One countermeasure is based on using high power laser (HPL) to destroy them. We report part of the numerical simulations of optimizing the duty cycle of a drone/UAV destruction laser. The main task was to determine the temperature distribution over the area of the fuselage targeted by the laser in order to discover the laser parameters needed to melt the fuselage and make a hole through the fuselage. The simulations were performed for zero to infinite thicknesses and in motion and represented the input data.

(Received July 16, 2024; accepted July 30, 2024)

Keywords: High-power fiber laser (HPFL), Drone/UAV simulation, Laser beam, Composite material, Grating fiber optic, Microphone sensor

1. Introduction

After about a decade of research it appears that the time has come to consider the path of laser weapons, which can destroy enemy drones and aircraft without the need to resort to expensive missiles, thus turning attention to lasers as a weapon system for defense anti-aircraft. Lasers have the great advantage of running on electricity and can therefore be powered by a ship's turbine engines.

High-Power Fiber Laser (HPFL) are utilizing a high-power laser in the 910nm to 980nm range to excite ions in rare earth elements such as ytterbium [1] or erbium which have been doped into fiber. The doped fiber then generates photons at longer wavelengths (in the infrared) propagating through the fiber itself (976 nm, 915 nm).

A laser diode is used to pump an HPFL, which can be: single emitter laser diodes offer up to roughly 12 watts of optical output power. To get higher power levels, two packaging approaches are used to combine multiple single emitter beams into one single high power output beam. These two approaches are bars and multi-single chip emitter modules. The terms "bar" and "array" are typically interchangeable. Both of these technology and packaging approaches have their advantages and disadvantages. But over the past few years, multi-single chip emitter modules have become increasingly more common due to the lower manufacturing costs and a perception that they may offer better long-term reliability.

Power-scaling of ytterbium (Yb³⁺)-doped single-fiber lasers (YDFL's) has now led to output powers beyond 1 kW. This rapid progress has been fueled both by the exceptional ability of fibers to carry high optical power and the availability of powerful diode lasers for use as pumps. These in turn are due mainly to improvements in fiber design and fabrication, and in multi-emitter lasers diodes, diode bars, and diode stacks [2].

As with other rare-earth doped silica fibers, YDFL's can be made tunable over several tens of nanometers, while one can access a wide range of wavelengths from the near

infrared to the so-called eye-safe region using other dopants, in particular neodymium (Nd³⁺) [3], erbium (Er³⁺), and thulium (Tm³⁺).

In the literature, efficiencies ranging from 64% to 83% have been reported for ytterbium-doped large-core fiber lasers. The fiber oscillators with direct diode pumping are highly efficient and have optical slope efficiencies from 64% at 1007nm to 83% at 1100nm relative to total laser diode pump power. [4 - 6].

Single-mode kW-level Yb fiber lasers [1] at wavelengths in the spectral range 1000 -1030nm with diffraction limited beam and direct diode pumping are outstanding sources of high brightness and low quantum defect for tandem pumping of fiber laser systems and multi-kilowatt crystal [7]. These full format SM Yb fiber lasers reach powers of 0.75kW, 0.90kW, 1.33kW and 1.40kW at 1007nm, 1010nm, 1018nm and 1030nm respectively with M² values < 1 output beam [5].

To investigate the limitations of SRS and SBS nonlinearities [8] at the peak power available in single-mode fiber lasers, various technical means have been developed to overcome the limitations. As a result, a feasibility of 100kW peak power at 5 ns pulse duration and 20 W average power with near TEM₀₀ output beam quality was achieved for the ytterbium fiber laser with a MOPFA configuration [9].

The study of drones/UAVs in flight for military applications, with light metal fuselage and/or composite materials, is a novelty problem. This problem is given by the destruction of drones/UAV (unmanned aerial vehicle) [10, 11] in action based on the use of high-power laser (HPL). Following the FEM (finite element method) [12] numerical simulations carried out in this paper we can contribute information regarding the optimization of the functional cycle of a laser equipment investigated for the annihilation of drones/UAVs.

The High-Power Fiber Laser (HPFL) simulation model consists of four main sub-models: 1 - Target - UAV/drone

fuselage; 2 - Beam propagation; 3 - Adaptive transmission optics; 4 - The Yb fiber laser.

We report the results obtained in the simulation of the interaction of the laser beam with the drone/UAV surface fuselage (made of aluminum and several types of composite materials) was numerically simulated. An important issue was deducing the temperature distribution over the fuselage area hit by the laser beam to predict the laser parameters needed to heat the fuselage to the melting temperature (level 1 of the simulations) and then drill, in the shortest possible time, a hole through it (level 2 of simulations). The simulations were performed as the fuselage is infinite (thickness is zero at infinity) and moving relative to the incident laser beam served as input data. Calculations were performed on two axes by comparison with the spot diameter of the laser beam. The calculations were performed considering that the fuselage moves at a certain speed relative to the axis of the laser beam. The simulations were performed considering the aluminum fuselage for comparison with the composite material cases. Several types of composite materials were analyzed, including those from Kevlar foils. The developed simulation model allows an analysis of the role of the foils and the thickness of the epoxy resin layer (airframes made of carbon fiber materials, glass fiber composites or polycarbonates).

The developed model allows the calculation of isotherms inside the fuselage and the "melting time", defined as the time required to reach the melting temperature at a certain depth inside the fuselage material.

Two main types of laser emission were considered for the simulations: continuous wave (cw) or modulated (Q-switch regime or mode-locked laser operation regime) [13]. This feature of the simulation model makes possible a correlation between the minimum required values to be achieved by the laser beam for simultaneous propagation in open space and interaction with the drone/UAV fuselage. The simulations were performed using a self-developed software package based on MATLAB 2023a.

2. Theory and description

There is increased interest in countermeasures against drones/UAVs in flight for military applications, such as drones/UAVs with light metal and/or composite fuselages.

An investigated countermeasure is based on the use of high-power laser (HPL) to destroy drones/UAVs in action.

We report part of the numerical [14 - 17] finite-element method simulation results that were performed to optimize the duty cycle of a research laser equipment for the direct destruction of drones/UAVs.

Calculations were made on two axes by comparison with the spot diameter of the laser beam that can be changed (50 mm for these results, and the fuselage is considered to move at a speed of up to 50 m/s in a plane perpendicular to the beam axis laser, along the x-axis (relative velocity).

The simulations considered the aluminum fuselage for the comparison of composite materials.

Several types of composite materials [18 - 20] were analyzed, such as foils and epoxy resin layers (airframes made of carbon fiber materials, glass fiber composites or polycarbonates).

The developed model allows the calculation of isotherms [21] inside the fuselage and the "melting time", defined as the time required to reach the melting temperature at a certain depth inside the fuselage material.

It is presented in Fig. 1 the practical realization of a high-power fiber laser is determined by the functional block diagram of a high-power fiber laser equipment for drone/UAV destruction. The component blocks of figure 1 are:

1-Power Source; 2-High Power Laser; 3-Beam Splitter; 4-Plane Controlled Deformable Mirror; 5-Telescope; 6-Beam Splitter; 7-Laser Beam Phase Detector; 8-Reference Laser; 9-Electronic Command Block; 10-Telescope Electronic Command Block; 11-Target

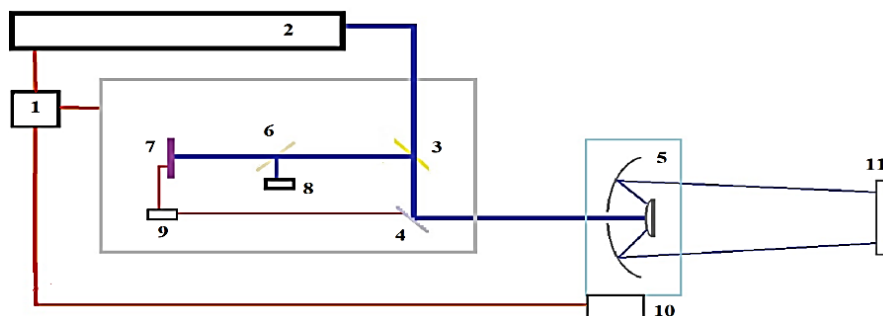


Fig. 1. Diagram of the high-power fiber laser equipment for drones/UAV annihilation. (Electrical connections are colored in red; Laser beam ray path is colored dark blue) (color online)

For simulations was considered laser emission: continuous wave (cw).

The High-Power Fiber Laser (HPFL) Simulation Model consists of four main sub-models:

1 - Target - UAV/drone fuselage. For this submodule, an important problem is the lack of knowledge of the

material from which the drone is made. Here the adjustment of the laser power level is an important factor.

2 - Beam propagation.

3 - Adaptive transmission optics.

4 - The Yb fiber laser.

An HPFL (High Power Fiber Laser) system for destroying drones in flight at distances of up to 10 km works

as an automatic, self-adjusting system, taking into account the characteristics of the atmosphere in the area where the drone is located, i.e.: humidity, wind speed, temperature of the environment in which the drone is located, etc.

These can be assessed to some extent using an attached LIDAR device.

In the simulations, the wavelength of the laser beam was 1076 nm (ytterbium fiber laser wavelength), a transverse Gaussian distribution of the laser intensity with different spot diameters.

The wavelength of the laser beam was chosen due to the good transmission of electromagnetic waves in air at this wavelength. Another issue to consider is the best possible adhesion (coupling) of the laser beam to the surface of the target material to heat and melt it.

It is worth noting that the developed simulation code relies on several initial approximations, including the neglect of vaporization due to the specific heat of the target material. For a first evaluation of the high-power laser to

destroy drones/ (UAV destruction system), this approximation can be considered acceptable.

The simulation code, developed, of the temperature of the target surface is of great importance characteristic, namely: the possibility to define the isothermal surface inside the target at different times after the start of laser heating and the permission to move the target in a direction transverse to the axis of the laser beam at speeds different.

In analyze of the high-power laser system for drone/UAV annihilation, two main types of lasers were investigated: Ytterbium fiber laser oscillator and amplifier and Ytterbium disk laser oscillator and amplifier.

For a better understanding of the phenomenon of the adhesion (coupling) of the laser beam with the fuselage of the drone/UAV, we present in figure 2 the simulations of the distribution of the laser beam intensity on the surface of the drone/UAV fuselage, by investigating the Ytterbium fiber optic laser for two distribution lengths of the laser beam on the drone/UAV fuselage: 5cm (Fig. 2 (a)) and 10cm (Fig. 2(b)).

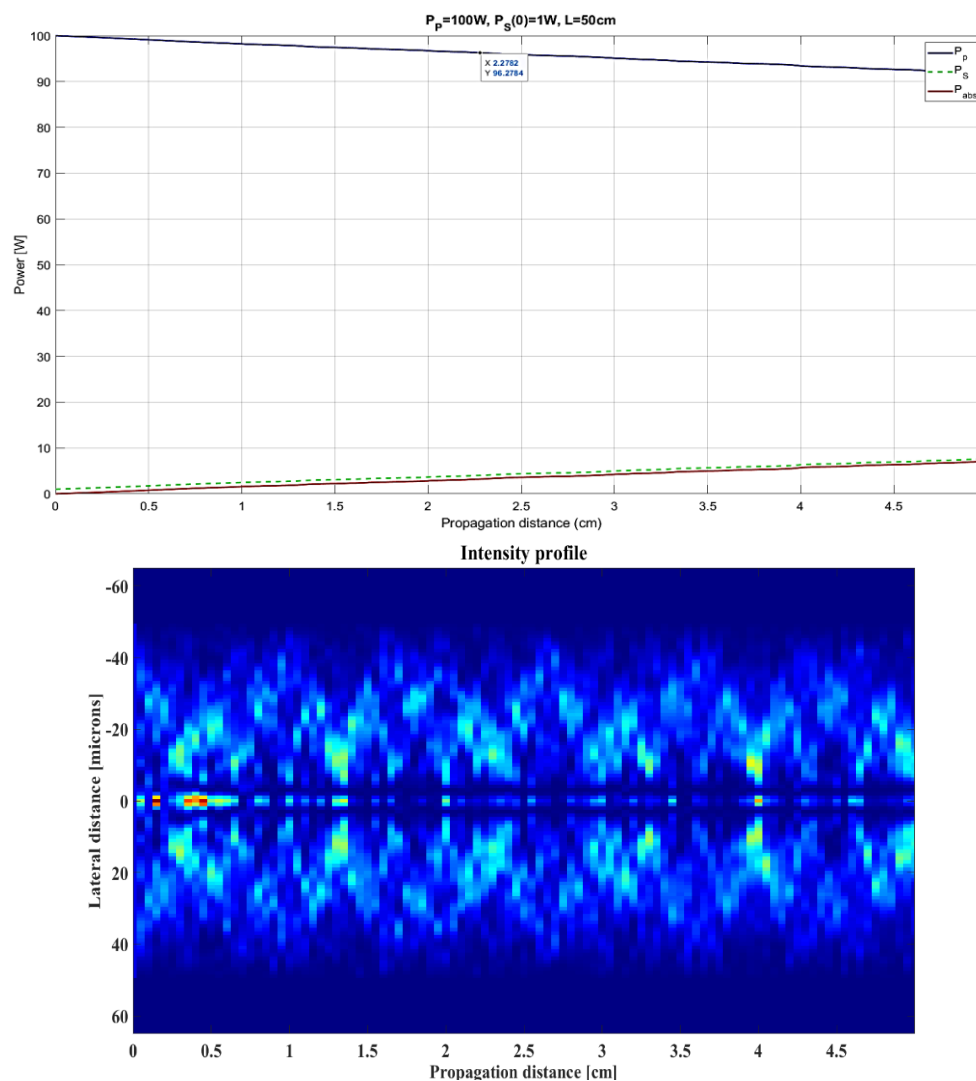


Fig. 2 (a) Example of laser beam distribution simulation on the surface of the drone/UAV fuselage; Ytterbium optic fiber - power signal, P_s increase as propagation along 5 cm length of optic fiber. (left); - longitudinal section of laser pulse electric field distribution (right) (color online)

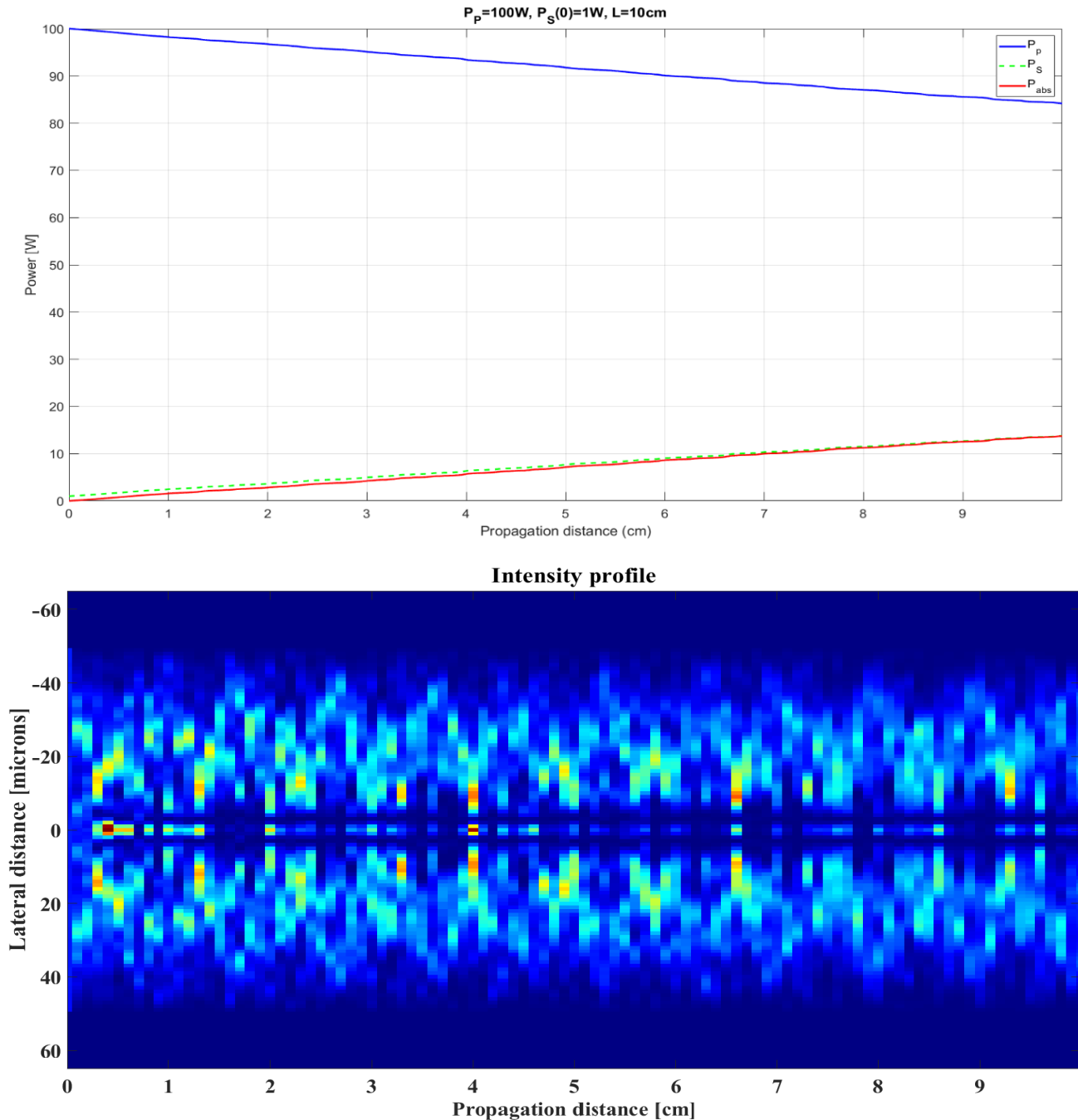


Fig. 2 (b). Example of laser beam distribution simulation on the surface of the drone/UAV fuselage; Ytterbium fiber optic - power signal, P_s increase as propagation along 10 cm length of optic fiber. (left); - longitudinal section of laser pulse electric field distribution (right) (color online)

3. Simulation results

In the following graphs are presented into 3D plots in Aluminum fuselage (5 figures) (of different thickness 10 mm, 20 mm) the temperature distribution on the target surface, $z = 0$, simulated for 5kW, 10kW, 15kW, 30kW and 45kW incident laser beam power.

The laser beam transverse distribution spot diameter was 50 mm. The target relative speed versus laser beam axis used in these simulations was of 2.7 m/s for all fuselage materials.

Similar temperature distributions but with lower maximum temperature were simulated for laser beam powers of 5kW, 10kW, 15 kW, 30kW and 45kW in carbon fiber reinforced composite, fiber glass and polycarbonates composite materials of 20 mm thickness [22].

In the presented graphs it can be noticed that for 45kW and Aluminum fuselage of 10 mm thickness maximum temperature achieved is 500°K lower than melting point of 660°C; for Carbon Fiber Composite fuselage of 20 mm thickness 7000°K was achieved higher than (~3650°C) melting temperatures; for fiber glass 80000°K can be

achieved, while for polycarbonates fuselage of 20 mm thickness, 2.2×10^5 K can be achieved.

3.1. Simulations on aluminum made UAV/drones

Simulations were performed with incident laser power levels of 5, 10, 15, 30 and 45 kW and spot diameter of 50 mm. For 45kW, the results are shown in Fig. 3. Simulations were performed for UAVs/drones flying at different "relative speeds" to the laser beam axis.

It is worth noting that at a "relative velocity" of less than 0.5 m/s, it was possible to simulate the laser heating of the aluminum target to the melting temperature at 2 mm depth at 22.5 kW, as well as for 45 kW of laser power incident on the target. The simulations are carried out for the flight axis of the drones perpendicular to the laser beam and relative speed of 2.7 m/s.

3.2. Simulations on composite made UAV/drones

Simulations were performed with incident laser power levels of 5, 10, 15, 30 and 45 kW and spot diameter of 50

mm. For the incident laser power of 45kW, the results are shown in Fig. 4 (carbon fiber), Fig. 5 (glass fiber) and Fig. 6 (polycarbonates). Simulations were performed for UAVs/drones flying at different "relative speeds" to the laser beam axis.

It is worth noting that even at a "relative velocity" of 2.7 m/s, it was possible to simulate the laser heating of the composite target to the melting temperature at 2 mm depth at an incident laser power on the target of less than 5kW.

It is worth noting that even at a "relative speed" of more than 0.5 m/s, it was possible to simulate the laser heating of the targeted composite structures to the formation of plasma, the beginning of other drone/UAV annihilation processes.

The fuselage of the drone is destroyed at ~4.5 kW.

Table 1 shows the melting temperature of the drone fuselage depending on the incident power of the laser and the material from which the fuselage is made (incident laser power levels of 5kW, 10kW, 15kW, 30kW).

Table 1. The melting temperature of the drone fuselage

The material from which the fuselage is made	Incident Laser Power			
	5kW	10kW	15kW	30kW
<u>ALUMINUM</u> "Melting time"/ on 10 mm fuselage thickness: ~10 μ s [calculated at 2.7 m/s Relative Speed for 125kW Incident Laser Power -Not a practical situation]	55°K	110°K	160°K	350°K
<u>CARBON FIBER</u> "Melting time"/ on 20 mm fuselage thickness: ~250 μ s [calculated at 2.7 m/s Relative Speed for 10kW Incident Laser Power -A practical situation].	800°K	1600°K	2000°K	2000°K
<u>FIBER GLASS</u> "Melting time"/ on 20 mm fuselage thickness: ~350 μ s [calculated at 2.7 m/s Relative Speed for 10kW Incident Laser Power -A practical situation].	8000°K	16000°K	20000°K	50000°K
<u>POLYCARBONATES</u> "Melting time"/ on 20 mm fuselage thickness: ~150 μ s [calculated at 2.7 m/s Relative Speed for 10kW Incident Laser Power -A practical situation].	20000°K	45000°K	70000°K	140000°K

3.3. Aluminum – 45 kW - Incident Laser Power (Fig. 3).

Relative Speed: 2.7 m/s -Drone speed flying on x-axis into a plane normal to laser beam.

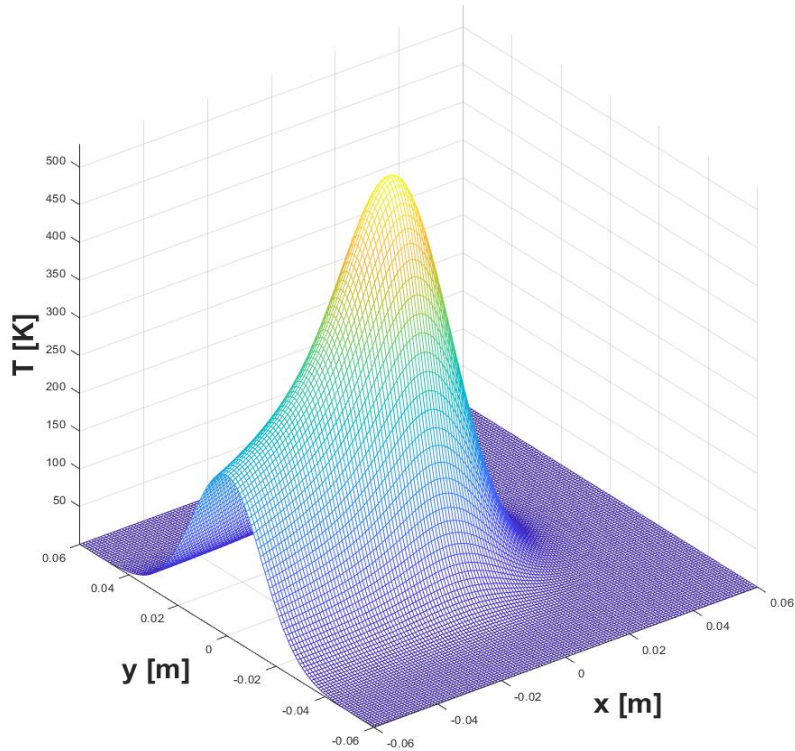
Figure on Left side: 3D representation of temperature on Drone surface. Maximum temperature: 500°K [relative to initial state].

Figure on Right side: Isotherms in a plane parallel to x-axis situated at $y = 0.00047244$ m.

The effect of Drone movement on x-axis can be noticed.

"Melting time"/ on 10 mm fuselage thickness: ~10 μ s [calculated at 2.7 m/s Relative Speed for 125kW Incident Laser Power - Not a practical situation].

Aluminum – 45 kW – Temperature profile @ z=0m



**Aluminum – 45 kW
Isotherms x-cross section @ y= -0.00047244m**

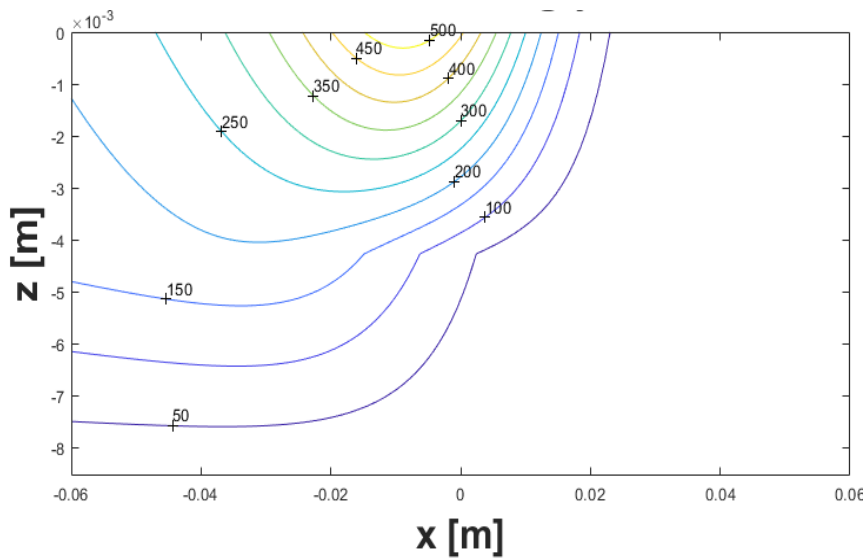


Fig. 3. Aluminum – 45 kW; 3D representation of temperature on Drone surface (left); Isotherms in a plane parallel to x-axis (right) (color online)

3.4. Carbon fiber – 45 kW - Incident Laser Power (Fig. 4).

Relative Speed: 2.7 m/s -Drone speed flying on x-axis into a plane normal to laser beam.

Figure on Left side: 3D representation of temperature on Drone surface. Maximum temperature: 7000°K [relative to initial state].

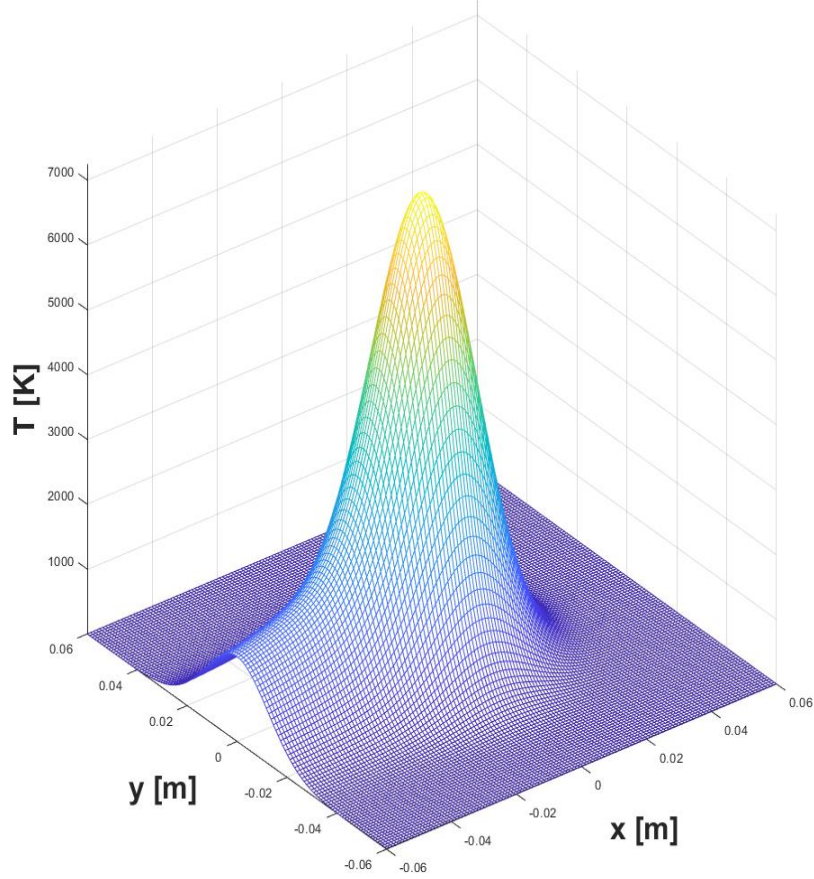
Figure on Right side: Isotherms in a plane parallel to x-axis situated at y = 0.00047244m.

The effect of Drone movement on x-axis can be noticed.

“Melting time”/ on 20 mm fuselage thickness: $\sim 250 \mu\text{s}$
 [calculated at 2.7 m/s Relative Speed for 10kW Incident
 Laser Power -A practical situation].

The Drone fuselage is destroyed at $\sim 4.5 \text{ kW}$.

Carbon Fiber - 45 kW - Temperature profile @ $z=0\text{m}$



Carbon Fiber - 45 kW Isotherms x-cross section @ $y=-0.00047244\text{m}$

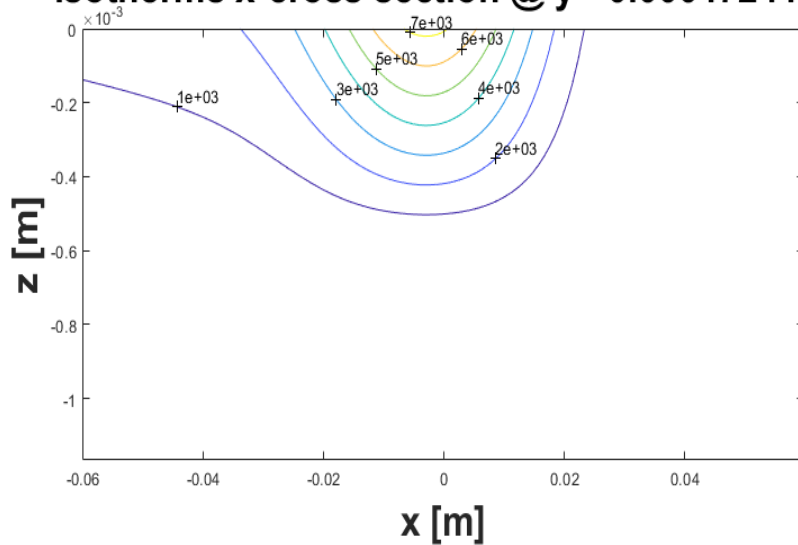


Fig. 4. Carbon fiber - 45 kW; 3D representation of temperature on drone surface (left); Isotherms in a plane parallel to x -axis (right) (color online)

3.5. Fiber glass – 45 kW - Incident Laser Power (Fig. 5).

Relative Speed: 2.7 m/s -Drone speed flying on x-axis into a plane normal to laser beam.

Figure on Left side: 3D representation of temperature on Drone surface. Maximum temperature: 80000°K [relative to initial state].

Figure on Right side: Isotherms in a plane parallel to x-axis situated at $y = 0.00047244\text{m}$.

The effect of Drone movement on x-axis can be noticed.

“Melting time”/ on 20 mm fuselage thickness: $\sim 350\ \mu$ [calculated at 2.7 m/s Relative Speed for 10 kW Incident Laser Power -A practical situation].

The Drone fuselage is destroyed at $\sim 3.5\ \text{kW}$ in a very short time.

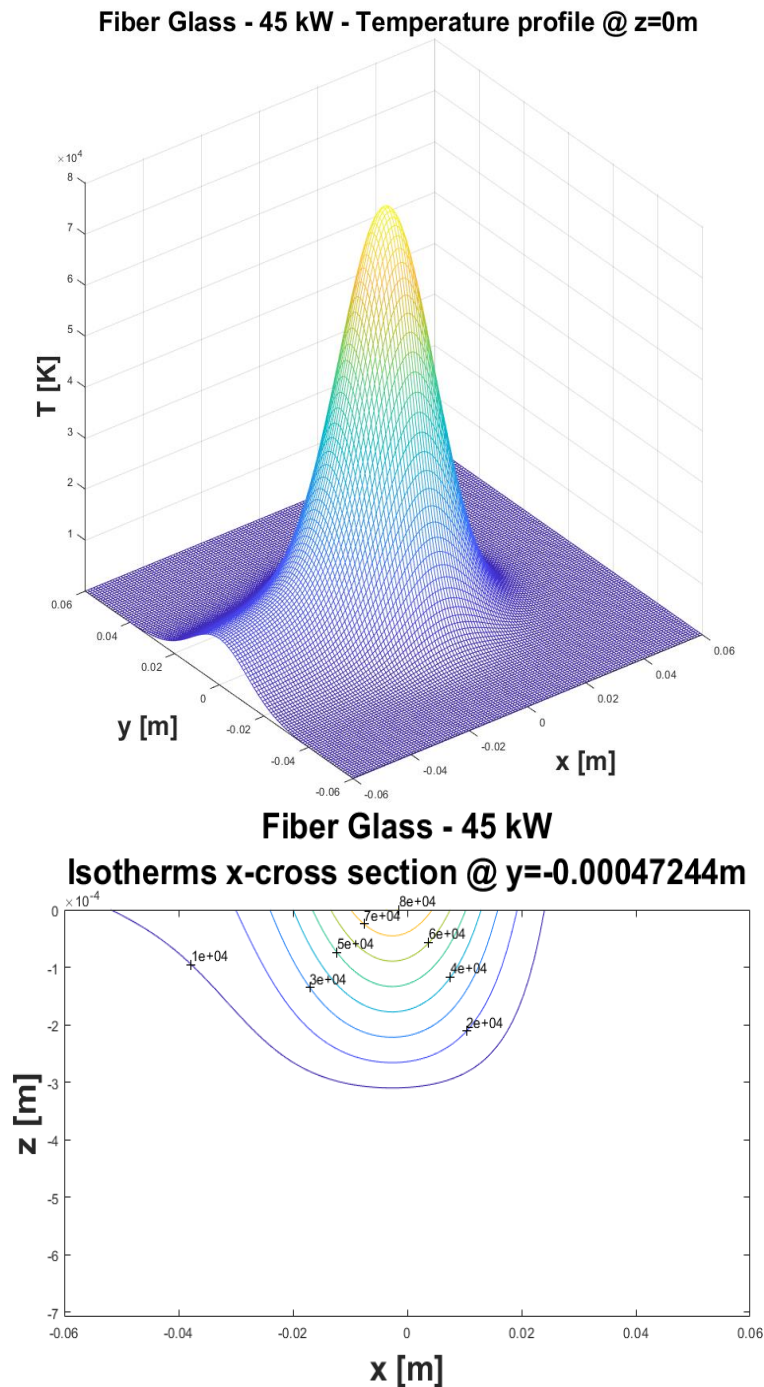


Fig. 5. Fiber glass - 45 kW; 3D representation of temperature on Drone surface (left); Isotherms in a plane parallel to x-axis (right) (color online)

3.6. Polycarbonates – 45 kW - Incident Laser Power (Fig. 6).

Relative Speed: 2.7 m/s -Drone speed flying on x-axis into a plane normal to laser beam.

Figure on Left side: 3D representation of temperature on Drone surface. Maximum temperature: 140000°K [relative to initial state].

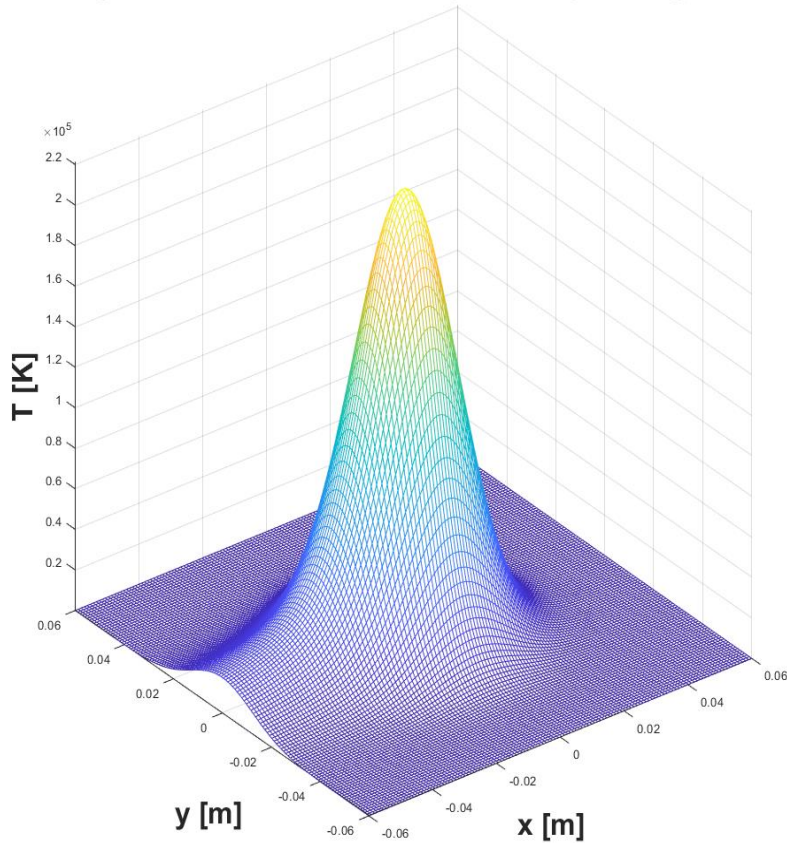
Figure on Right side: Isotherms in a plane parallel to x-axis situated at $y = 0.00047244\text{m}$.

The effect of Drone movement on x-axis can be noticed.

“Melting time”/ on 20 mm fuselage thickness: ~350 ms [calculated at 2.7 m/s Relative Speed for 10 kW Incident Laser Power -A practical situation].

The Drone fuselage is destroyed at ~2.5 kW in a very short time.

Polycarbonates - 45 kW -Temperature profile @ z=0m



Polycarbonates - 45 kW Isotherms x-cross section @ y=-0.00047244m

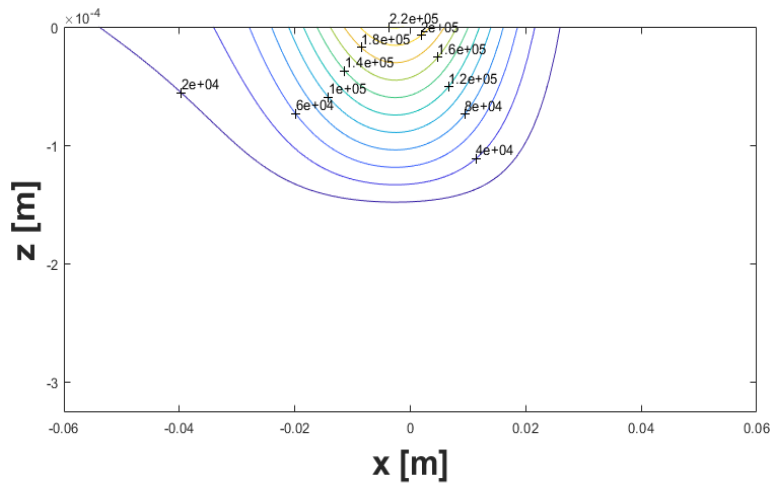


Fig. 6. Polycarbonates –45 kW; 3D representation of temperature on drone surface (left); Isotherms in a plane parallel to x-axis (right) (color online)

4. Conclusions

For the authors, the presented results represent the first stage of simulating the interaction of a high power 45kW fiber optic laser with the surface of the fuselage of a drone/UVA with a military application in order to destroy it. This first stage mainly consists of creating software packages of codes that cover possible applications. Future research directions resulting from the said study will be reported when and together with the experimental results obtained.

There are presented results obtained in simulation of In-flight drones/UAV with fuselage made of Light Metal and/or composite materials annihilation using a cw Ytterbium fiber laser OPERATED at 1076 nm and output power up to 50kW.

The results are obtained using a finite-element method simulation model.

The presented results are of the 1st level simulations concerning only the temperature distribution on fuselage zone on which the laser beam is incident, investigating if melting temperature is reached.

Calculations were performed on two axes by comparison with the laser beam spot diameter which can be modified (50 mm) for the presented results.

Calculations were performed considering that the fuselage is moving with a speed up to 50 m/s in a plane perpendicular to the laser beam axis, along x axis (Denoted as relative speed).

Simulations were performed considering aluminum made fuselage for comparison versus the cases of composite materials.

Several types of composite materials were analyzed, including the ones made of foils and epoxy resin layer (fuselages made of carbon fiber-based materials, fiber glass composites or polycarbonates).

The developed model allows calculation of isotherms inside fuselage and of “melting time”, defined as the time necessary to obtain melting temperature at a certain depth inside fuselage material.

Simulation allows several main observations/conclusions to be noticed:

– for an aluminum made fuselage moving with greater than 5 m/s speed relative to laser beam axis, the melting temperature is impossible to be achieved, even using a 50-kW laser power;

– for composite made fuselage, because of its lower thermal diffusivity, even at 10 – 15 kW laser power, a temperature corresponding to significant composite thermal & mechanical status modification, can be obtained.

Acknowledgements

This work was supported by the Core Program within the National Research Development and Innovation Plan 2022-2027, carried out with the support of MCID, project no. PN 23 05, the Romanian Ministry of Research, Innovation and Digitalization, and a grant of the Ministry of Research, Innovation and Digitalization, CNSC-

UEFISCDI, project number PN-III-P4-PCE-2021-0585, within PNCDI III.

References

- [1] Yoon-Chan Jeong, Alexander J. Boyland, Jayanta Sahu, Seung-Hwan Chung, Johan Nilsson, David N. Payne, *Journal of the Optical Society of Korea* **13**(4), 416 (2009).
- [2] Y. Jeong, J. K. Sahu, D. N. Payne, J. Nilsson, *Optics Express* **12**(25), 6088 (2004).
- [3] K.-I. Ueda, H. Sekiguchi, H. Kan, *Proc. Conference on Lasers and Electro-Optics 2002*, Long Beach, USA, 2002.
- [4] Y. Jeong, J. K. Sahu, D. N. Payne, J. Nilsson, *Advanced Solid-State Photonics, OSA Technical Digest* (Optica Publishing Group, 2004), paper PDP13.
- [5] Nikolai Platonov, Oleg Shkurikhin, Valentin Fomin, Daniil Myasnikov, Roman Yagodkin, Anton Ferin, Alexey Doronkin, Ivan Ulyanov, Valentin Gapontsev, *Proc. SPIE* **11260**, *Fiber Lasers XVII: Technology and Systems*, 1126003 (2020).
- [6] Y. Jeong, J. K. Sahu, D. N. Payne, J. Nilsson, *Optics Express* **12**(25), 6088 (2004)..
- [7] W. Wei, J. Duan, Y. Yang, G. Qin, *J. Optoelectron. Adv. M.* **26**(5-6), 173 (2024).
- [8] Rahul Umesh Kale, Pavan Mahadeo Ingale, Rameshwar Tukaram Murade, *International Journal of Recent Technology and Engineering (IJRTE)* **2**(1), 61825637 (2013).
- [9] Valentin P. Gapontsev, Valentin Fomin, Andrei Ount, Igor E. Samartsev, *Proc. SPIE* **3613**, *Solid State Lasers VIII*, (1999).
- [10] Zhu Xiaoning, *IEEE Xplore*, 3rd International Conference on Unmanned Systems (ICUS), 2020.
- [11] Kim Hartmann, Keir Giles, *IEEE Xplore*, 8th International Conference on Cyber Conflict (CyCon), 2016.
- [12] He Jianli, *Optoelectron. Adv. Mat.* **15**(1-2), 11 (2021).
- [13] Zengrun Wen, Xiulin Fan, Kaile Wang, Weiming Wang, Song Gao, Wenjing Hao, Yuanmei Gao, Yangjian Cai, Liren Zheng, *arXiv:2302.12046*.
- [14] D. Savastru, S. Miclos, R. Savastru, I. Lancranjan, *Proc SPIE Int. Soc. Opt. Eng.* **9517**, 95172A (2015).
- [15] S. Miclos, D. Savastru, R. Savastru, I. Lancranjan, *Compos. Struct.* **183**, 521 (2018).
- [16] I. Lancranjan, D. Savastru, S. Miclos, A. Popescu, *J. Optoelectron. Adv. M.* **12**(12), 2456 (2010).
- [17] S. Miclos, D. Savastru, I. Lancranjan, *Rom. Rep. Phys.* **62**(3), 519 (2010).
- [18] D. Savastru, S. Miclos, R. Savastru,

- I. Lancranjan, *Compos. Struct.* **183**, 682 (2018).
- [19] D. Savastru, S. Miclos, R. Savastru, I. Lancranjan, *Compos. Struct.* **226**, 1243 (2019).
- [20] S. Miclos, D. Savastru, R. Savastru, I. Lancranjan, *Compos. Struct.* **218**, 15 (2019).
- [21] Risti Ragadhita, Asep Nandiyanto, *Ijost Ijost, Indonesian Journal of Science and Technology* **6**(1), 205 (2021).
- [22] Min Zhou, Qingmeng Zhang, Feihu Tan, Junyou Chen, Zhuye Sun, *Optoelectron. Adv. Mat.* **13**(11-12), 609 (2019).

*Corresponding authors: savuv@inoe.ro;
madalin@inoe.ro